The Full-length *Saccharomyces cerevisiae* Sgs1 Protein Is a Vigorous DNA Helicase That Preferentially Unwinds Holliday Junctions*

Petr Cejka and Stephen C. Kowalczykowski[1]

From the Departments of Microbiology and Molecular and Cellular Biology, University of California, Davis, California 95616-8665

The highly conserved RecQ family of DNA helicases has multiple roles in the maintenance of genome stability. Sgs1, the single RecQ homologue in *Saccharomyces cerevisiae*, acts both early and late during homologous recombination. Here we present the expression, purification, and biochemical analysis of full-length Sgs1. Unlike the truncated form of Sgs1 characterized previously, full-length Sgs1 binds diverse single-stranded and double-stranded DNA substrates, including DNA duplexes with 5′- and 3′-single-stranded DNA overhangs. Similarly, Sgs1 unwinds a variety of DNA substrates, including blunt-ended duplex DNA. Significantly, a substrate containing a Holliday junction is unwound most efficiently. DNA unwinding is catalytic, requires ATP, and is stimulated by replication protein A. Unlike RecQ homologues from multicellular organisms, Sgs1 is remarkably active at picomolar concentrations and can efficiently unwind duplex DNA molecules as long as 23,000 base pairs. Our analysis shows that Sgs1 resembles *Escherichia coli* RecQ protein more than any of the human RecQ homologues with regard to its helicase activity. The full-length recombinant protein will be invaluable for further investigation of Sgs1 biochemistry.

DNA helicases are ATP hydrolysis-driven translocases that separate the two strands of duplex DNA. They are found in all living organisms and perform essential functions during replication, transcription, and repair of DNA. The RecQ family belongs to superfamily 2 of helicases, which was named after the founding member from *Escherichia coli* (1). Budding yeast, *Saccharomyces cerevisiae*, possesses a solitary RecQ helicase, Sgs1 (2, 3). Strains deleted for *SGS1* are sensitive to genotoxic agents, such as methylmethane sulfonate, have reduced life span, show increased chromosome missegregation, and display mitotic hyperrecombination phenotype. Whereas most prokaryotes and unicellular eukaryotes express a single RecQ homologue, multicellular eukaryotic organisms possess several family members (reviewed in Ref. 4).

The general interest in this group of helicases was raised after the discovery that mutations in at least three of the five human homologues, BLM, WRN, and RECQ4, are linked to genetic disorders (5–7). When mutated, the resultant genetic abnormality causes Bloom, Werner, and Rothmund-Thompson syndromes, respectively. The affected individuals are characterized by a rapid onset of cancer, accelerated aging, growth abnormalities, and other defects (reviewed in Ref. 8). At the cellular level, the RecQ proteins maintain genomic stability through various mechanisms, including important roles at various steps of double-stranded DNA (dsDNA)[2] break repair (9).

In *E. coli*, the RecQ protein is a helicase that acts on both partially and fully duplex DNA (10). It initiates homologous recombination via the RecF pathway by processing a dsDNA molecule to provide a 3′-terminated single-stranded (ssDNA) that is used by the RecA protein for homologous pairing (11, 12). The RecF pathway is the major homologous recombination pathway for ssDNA gap repair, and in the absence of the RecBCD enzyme, the RecF pathway can completely assume the responsibility for the repair of dsDNA breaks (reviewed in Refs. 13 and 14). Because RecQ can act on a wider variety of DNA substrates than RecBCD (11), it can initiate homologous recombination on substrates that are not suitable for RecBCD (14–16). Moreover, not only can the RecQ helicase promote recombination, but it can also disrupt joint molecule intermediates *in vitro* (11, 13), thereby contributing to recombination fidelity (17) and to recombinational repair without crossing over. Finally, RecQ has the unique capacity to functionally interact with topoisomerase III to promote the catenation and decatenation of dsDNA (18–20).

A number of these characteristics are conserved among eukaryotic homologues. Mutation of *S. cerevisiae SGS1* rescues the slow growth phenotype of strains lacking topoisomerase III (Top3), and both factors interact genetically and physically (2). The *sgs1Δ*, *top3Δ*, and *sgs1Δ top3Δ* mutants accumulate recombination-dependent cruciform structures at replication forks that encountered a damaged template (21). Human and *Drosophila* BLM also interact with their cognate topoisomerase, Topo IIIα, *in vitro* (9). The heterodimer can migrate and "dissolve" the double Holliday junctions that arise during homologous recombination, producing non-crossover recombination products (22–24).

In addition to processing of recombination intermediates by dissolution, *Drosophila* BLM promotes synthesis-dependent

---

[1] To whom correspondence should be addressed: Dept. of Microbiology, University of California, Davis, One Shields Ave., Davis, CA 95616-8665. Tel.: 530-752-5938; Fax: 530-752-5939; E-mail: sckowalczykowski@ucdavis.edu.

[2] The abbreviations used are: dsDNA, double-stranded DNA; HRDC, helicase and RNase D C-terminal; MBP, maltose-binding protein; nt, nucleotide(s); RPA, replication protein A; ssDNA, single-stranded DNA; SSB, single-stranded DNA-binding protein; PMSF, phenylmethanesulfonyl fluoride; NTA, nitrilotriacetic acid.

strand annealing (SDSA), a recombination pathway that also leads to non-crossover products (25). RecQ family members are also believed to suppress illegitimate recombination by unwinding aberrantly paired DNA molecules at regions of limited homology (17, 26). Finally, very recently, both human (BLM) and yeast (Sgs1) RecQ homologues were shown to promote 5′-end resection at dsDNA break sites to form 3′-ssDNA tails, a key early step in homologous recombination (27–30).

Although all RecQ helicases unwind DNA with a 3′→5′ polarity, they differ markedly with respect to activity and substrate specificity. The *E. coli* RecQ helicase is active on a wide variety of duplex DNA substrates (11), whereas the multicellular eukaryotic RecQ homologues are typically less robust, and each has apparently specialized to bind and unwind distinct structures (31–35). Our understanding of the function of the yeast Sgs1 helicase is based almost exclusively on genetic studies because attempts to obtain full-length protein were unsuccessful (36). The existing biochemical analyses used only the central Sgs1 fragment containing residues 400–1268, whereas the full-length protein comprises 1447 amino acids. This fragment of Sgs1, containing the helicase domain, has strong preference for binding and unwinding DNA substrates with 3′-ssDNA tails (36, 37). However, the missing N- and C-terminal domains mediate interactions with the binding partners Top3 (2) and Rad51 (38), respectively, which are important to function *in vivo*. Moreover, the missing domains might mediate additional interactions with DNA and, thus, contribute to substrate binding interactions. Specifically, the Sgs1 fragment lacks the helicase and RNase D C-terminal (HRDC) domain implicated in conferring DNA substrate specificity (39, 40). The HRDC domain in BLM is essential for dissolution of double Holliday junctions (24), implying that the full-length Sgs1 will be indispensable for proper mechanistic analysis.

In this study, we expressed and purified full-length Sgs1 protein using the baculovirus expression system. We demonstrate that the recombinant protein possesses unexpectedly high levels of ATPase and helicase activities and that it can unwind a wide variety of duplex DNA molecules. Notably, the full-length Sgs1 helicase shows a marked preference for unwinding DNA with a Holliday junction.

EXPERIMENTAL PROCEDURES

Expression Plasmids—The sequence coding for both the maltose-binding protein (MBP) tag and PreScission protease cleavage site was amplified by PCR using pMal-P vector (modified pMal-c2x vector from New England Biolabs) as the DNA template and DNA oligonucleotides PC11 (CGCAAATCGGATC-CCATATGATGAAAATCGAAGAAGGTAAACTG; BamHI site underlined) and PC12 (CGCAAATCGCTAGCGGGC-CCCTGGAACAGAACTTCCAG; NheI site underlined). The PCR product was then digested with BamHI and NheI restriction endonucleases and cloned into the BamHI and NheI restriction sites in pFB-GST-BLMh10 (22), creating pFB-MBP-BLMh10. The sequence coding for the glutathione *S*-transferase tag was replaced by that coding for the MBP tag in this step. Next, the *SGS1* coding sequence was amplified by PCR using DNA oligonucleotides PC1 (CTCTGAACTCGAGCTGGAA-GTTCTGTTCCAGGGGCCCGCTAGCGGATCCATGGTG-

ACGAAGCCGTCACATAAC; NheI site underlined) and PC2 (CGCAAATCCTCGAGCCCGGGTCACTTTCTTCCTCTG-TAGTGAC; XhoI site underlined) and *S. cerevisiae* wild type genomic DNA (strain S288C, Research Genetics). The reaction product was digested by NheI and XhoI endonucleases and cloned into pFB-MBP-BLMh10, creating pFB-MBP-Sgs1. The sequence of the *Dm*BLM gene was replaced by that of full-length *SGS1* in this step. Finally, the sequence coding for the C terminus of *SGS1* was amplified by PCR using oligonucleotides PC55 (CGGCTTCCAGCAATGGGATTGC) and PC56 (CGC-AAATCCTCGAGCCCGGGTCA**ATGGTGATGGTGATG-GTGATGGTGATGGTG**CTTTCTTCCTCTGTAGTGAC; XhoI site underlined, sequence coding for decahistidine tag in boldface type). The amplified DNA fragment was digested by KasI and XhoI restriction endonucleases and cloned into KasI and XhoI sites in pFB-MBP-Sgs1. This step added the C-terminal decahistidine tag to the *SGS1* sequence, creating pFB-MBP-SGS1-His. The sequence of *SGS1* was verified by sequencing. The plasmid (pFB-MBP-SGS1K706A-His) coding for the ATPase-dead mutant, Sgs1 (K706A) was obtained by using QuikChange II XL site-directed mutagenesis kit (Stratagene) according to the manufacturer's recommendation, using the mutagenic primers PC57 (CTTATGCCAACAGGGGGTGG-CGCCTCTCTTTGCTATCAACTTC) and PC58 (GAAGT-TGATAGCAAAGAGAGGCGCCACCCCCTGTTGGCAT-AAG), and verifying the unique change by sequencing. All restriction endonucleases were purchased from New England Biolabs. The enzyme used for PCRs was ExTaq (Takara Bio).

Expression and Purification of Recombinant Proteins—MBP-Sgs1 protein was expressed using the pFB-MBP-Sgs1-His vector and the Bac-to-Bac baculovirus expression system (Invitrogen) in Sf9 cells, according to the manufacturer's recommendations. The protocol describes purification from 3.2 liters of Sf9 cell culture. Pellets of Sf9 cells expressing MBP-Sgs1 were frozen 52 h after viral infection and stored at −80 °C. All subsequent steps were performed on ice or at 4 °C. Cells were thawed and resuspended in 3 pellet volumes of lysis buffer (50 mM Tris-HCl, pH 7.5, 1 mM dithiothreitol, 1 mM EDTA, 1:400 protease inhibitor mixture (Sigma P8340), 1 mM phenylmethanesulfonyl fluoride (PMSF), 30 μg/ml leupeptin). Cells were incubated for 20 min with gentle agitation, and then 2 pellet volumes of ice-cold 50% glycerol were added to the sample. Next, 5 M NaCl (6.5% of the total solution volume) was added dropwise to the sample, and the solution was incubated for 30 min with gentle agitation. The soluble extract was obtained by pelleting the insoluble material at 58,000 × *g* for 30 min. Amylose resin (8 ml; New England Biolabs) was pre-equilibrated according to the manufacturer's recommendations in a disposable plastic column (Thermo Scientific) and batch-wise incubated with the cleared protein extract for 1 h. The resin was extensively washed batch-wise, at first, and then in the column with wash buffer (50 mM Tris-HCl, pH 7.5, 5 mM β-mercaptoethanol, 1 M NaCl, 10% glycerol, 1 mM PMSF, 10 μg/ml leupeptin). MBP-Sgs1 was eluted with 20 ml of elution buffer (50 mM Tris-HCl, pH 7.5, 5 mM β-mercaptoethanol, 300 mM NaCl, 10% glycerol, 1 mM PMSF, 10 μg/ml leupeptin, and 10 mM maltose). Protein concentration in the eluate was estimated using the Bradford method with bovine serum albumin as a protein

standard, and the recombinant PreScission protease was added to the sample (12 μg of protease per 100 μg of protein) to remove the MBP tag. The sample was incubated for 3 h. Next, 0.5 g of Bio-Rex70 resin (Bio-Rad) was pre-equilibrated with elution buffer, and batch-wise incubated with the sample for 15 min. Flow-through was collected by loading the slurry into a plastic disposable column, and imidazole was added to a final concentration of 20 mM. Ni^{2+}-NTA-agarose (1 ml; Qiagen) was pre-equilibrated with elution buffer supplemented with 20 mM imidazole, added to the sample, and incubated for 1 h. The sample was then applied on a disposable plastic column; washed with 20 ml of NTA buffer A1 (50 mM Tris-HCl, pH 7.5, 5 mM β-mercaptoethanol, 1 M NaCl, 10% glycerol, 1 mM PMSF, 10 μg/ml leupeptin, 58 mM imidazole) and 5 ml of NTA buffer A2 (50 mM Tris-HCl, pH 7.5, 5 mM β-mercaptoethanol, 150 mM NaCl, 10% glycerol, 1 mM PMSF, 10 μg/ml leupeptin, 58 mM imidazole); and eluted with 4 ml of NTA buffer B (50 mM Tris-HCl, pH 7.5, 5 mM β-mercaptoethanol, 150 mM NaCl, 10% glycerol, 1 mM PMSF, 10 μg/ml leupeptin, 400 mM imidazole). Sgs1 protein was then dialyzed overnight against 1 liter of dialysis buffer (50 mM Tris-HCl, pH 7.5, 5 mM β-mercaptoethanol, 300 mM NaCl, 50% glycerol, 0.5 mM PMSF, 1 μg/ml leupeptin), flash frozen in liquid nitrogen in small aliquots, and stored at $-80\,^{\circ}$C. Protein concentration was determined by the Bradford method, using bovine serum albumin as a protein standard. A typical purification yielded $\sim$100–200 μg of Sgs1 protein at a final concentration of $\sim$600–900 nM. The catalytically inactive Sgs1 (K706A) mutant was purified identically; the yield was 400 μg, and the final concentration was 1.54 μM. Sgs1 tested negative for nuclease contamination in reactions carried out in helicase buffer (see below) without ATP and with 10 mM magnesium acetate, on the Y-structure oligonucleotide substrate during a 60-min incubation at 30 °C. *E. coli* SSB and *S. cerevisiae* replication protein A (RPA) were purified as described previously (18, 41) and were shown to have the reported ssDNA binding stoichiometries.

Nucleic Acid Substrates—DNA oligonucleotides were purchased from Sigma, purified by polyacrylamide gel electrophoresis, and ^{32}P-labeled with T4 polynucleotide kinase (New England Biolabs) at their 5′-end, if necessary. Unincorporated nucleotides were removed using MicroSpin G25 columns (GE Healthcare). The substrates were prepared by heating the oligonucleotides at 95 °C and slow gradual cooling to room temperature in STE buffer (10 mM Tris-HCl, pH 7.5, 1 mM EDTA, and 100 mM NaCl). The sequences of the oligonucleotides were as follows: X12-3, GACGTCATAGACGATTACATTGCTA-GGACATGCTGTCTAGAGACTATCGC; X12-4 NC, GCGA-TAGTCTCTAGACAGCATGTCCTAGCAAGCCAGAATT-CGGCAGGCTA; X12-4 C, GCGATAGTCTCTAGACAGCA-TGTCCTAGCAATGTAATCGTCTATGACGTC; X12-3 SC, TTGCTAGGACATGCTGTCTAGAGACTATCGC; X12-4 SC, GCGATAGTCTCTAGACAGCATGTCCTAGCAA). The oligonucleotides that were radioactively labeled are indicated with an asterisk below. The Y-structure substrate contained a 31-bp dsDNA region and both 5′- and 3′-ssDNA arms 19 nucleotides (nt) in length, and it was prepared by annealing X12-3* and X12-4 NC oligonucleotides. The 3′-overhang substrate contained a 31-bp dsDNA region and a 3′-ssDNA 19-nt

tail, and it was prepared by annealing X12-3 SC* and X12-4 NC. The 5′-overhang substrate contained a 31-bp duplex region and a 5′-ssDNA 19-nt tail, and it was prepared by annealing X12-3* and X12-4 SC. The long dsDNA substrate was 50 bp in length, and it was prepared by annealing X12-3* and X12-4 C oligonucleotides. The short dsDNA substrate was 31 bp in length and was prepared by annealing of X12-3 SC* and X12-4 SC oligomers. The long ssDNA substrate was the 50-nt oligonucleotide, X12-3*, and the short single-stranded substrate was the 31-nt oligonucleotide, X12-3 SC*. The oligonucleotides used to prepare the single Holliday junction substrate were identical to those described previously (42).

Substrates using ϕX174 DNA were prepared by annealing a 66-nt oligomer, PC63 (AGTGTTAACTTCTGCGTCATGGA-AGCGATAAAACTCTGCAGGTTGGATACGCCAATCAT-TTTTATC), to ϕX174 virion ssDNA (New England Biolabs). The oligonucleotide is complementary to ϕX174 at nucleotides 5357–36 (36). To prepare the undigested, circular substrate, the PC63 oligonucleotide was ^{32}P-labeled at the 5′ terminus. To prepare the 5′-labeled linear substrate depicted in Fig. 7, the PC63 oligonucleotide was ^{32}P-labeled at the 5′ terminus and annealed to ϕX174, and the resulting duplex was digested with PstI. To prepare the linear 3′-labeled substrate, the PC63 oligonucleotide was first annealed to ϕX174, the duplex was digested with PstI, and the 3′-end was labeled using Klenow fragment of DNA polymerase I (New England Biolabs) and dGTP and [α-^{32}P]dATP nucleotides. The reaction resulted in extension of the duplex region by 4 nt.

Helicase Assays—Helicase assays (15-μl volume) were carried out with oligonucleotide-based substrates (0.15 nM molecules) or ϕX174-based substrates (1 nM molecules) in helicase buffer (20 mM Tris acetate, pH 7.5, 2 mM magnesium acetate, 2 mM dithiothreitol, 100 μg/ml bovine serum albumin, 2 mM ATP). Where indicated, the helicase buffer was supplemented with *E. coli* SSB or *S. cerevisiae* RPA, which were present at a 3-fold molar excess (with regard to saturation of the ssDNA upon complete unwinding reaction) for the oligonucleotide-based substrates, or a 1.5-fold molar excess for the ϕX174-based substrates. For each single-stranded binding protein, ssDNA saturation is defined by the DNA-binding site size ($\sim$16 nt/SSB monomer and $\sim$20 nt/trimeric RPA) (43, 44). Reactions were assembled on ice, briefly equilibrated at room temperature, and initiated by adding the indicated concentrations of Sgs1. Helicase assays with λ phage-based DNA substrates were carried out similarly to those with ϕX174-based substrates, except that the DNA substrate concentration was 0.05 nM molecules (per full-length λ DNA), and the ATP concentration in helicase buffer was 3 mM. Reactions were incubated for 30 min at 30 °C and terminated with 5 μl of stop buffer (150 mM EDTA, 2% SDS, 30% glycerol, 0.1% bromphenol blue) for 30 min at 30 °C. When the radioactively labeled oligonucleotide substrates was used, the stop buffer also contained a 20-fold concentration excess of the identical but unlabeled oligonucleotide, to prevent spontaneous reannealing of the unwound substrate strands after the reaction termination. Time course reactions were carried out identically, except the initial reaction volume was 150 μl, and 15-μl aliquots were added to 5 μl of stop buffer at the indicated time points. Products of the reac-

tions with oligonucleotide-based substrates were analyzed by 10% polyacrylamide (acrylamide/bisacrylamide ratio 19:1) gel electrophoresis in TBE buffer (89 mM Tris borate, 2 mM EDTA). Products of the reactions with ϕX174-based substrates were analyzed by 1% agarose gel electrophoresis in TAE buffer (40 mM Tris acetate, 1 mM EDTA, pH 8.4). The gels were then dried on DE 81 paper (Whatman), exposed to a storage phosphor screen, and scanned using a Storm imaging system (Molecular Dynamics). Data quantification was performed using Image-QuaNT software (Version 5.2, GE Healthcare).

Electrophoretic Mobility Shift Assays—The electrophoretic mobility shift assays to characterize the binding of Sgs1 to various DNA substrates (0.15 nM molecules) were carried out similarly to the helicase assays with oligonucleotide-based substrates, except that ATP was omitted from the binding buffer. The complexes were mixed with 3 μl of loading buffer (50% glycerol, 0.1% bromphenol blue) and were immediately analyzed by 6% polyacrylamide gel electrophoresis in TBE buffer at room temperature. Data were quantified using ImageQuaNT software based on the disappearance of the substrate band.

ATPase Assay—This assay was based on a reaction in which the regeneration of hydrolyzed ATP is coupled to the oxidation of NADH, which can be monitored spectrophotometrically in real time. The assay and data evaluation is described in Refs. 45 and 46. The reaction buffer contained the indicated concentrations of Sgs1 and, unless specified otherwise, 1 μM (nucleotides) nucleic acid cofactors, 1 mM ATP, 25 mM Tris acetate, pH 7.5, 1 mM magnesium acetate, 0.1 mM dithiothreitol, 1 mM phosphoenolpyruvate, 25 units/ml pyruvate kinase (Sigma), 25 units/ml L-lactate dehydrogenase (Sigma), and 200 μM NADH (Sigma). Reactions were assembled on ice, briefly equilibrated at 30 °C, and initiated by adding Sgs1. Control reactions contained all components except for Sgs1 and did not show any significant change in absorbance over the time course of the reaction. The kinetic parameters were calculated using Prism software (Version 5.0 for Mac, GraphPad Software).

RESULTS

Purification of Full-length Sgs1—The full-length *SGS1* gene was fused with the sequence coding for MBP to add an N-terminal affinity tag. The MBP sequence was separated from *SGS1* by a PreScission protease cleavage site. Full-length Sgs1 was expressed using the Bac-to-Bac expression system in Sf9 cells and purified by affinity chromatography using an amylose resin (which binds MBP-tagged proteins with high affinity). The initial purifications yielded full-length MBP-Sgs1 protein that contained large amounts of Sgs1 truncation products (data not shown). To circumvent this problem, we fused a decahistidine tag at the C terminus of the MBP-Sgs1 construct (Fig. 1A). The affinity tags did not alter the protein's ability to complement methylmethane sulfonate sensitivity of a *sgs1*Δ mutant when expressed from the yeast expression vector, pYES2 (data not shown). The fusion protein construct was expressed in Sf9 cells, and the MBP-Sgs1-His$_{10}$ was isolated first using amylose affinity chromatography. The MBP-tagged fusion protein was then cleaved by PreScission protease, and Sgs1 was further purified using Ni^{2+}-NTA-agarose (Qiagen). The full-length protein used for the biochemical characterization in this study con-
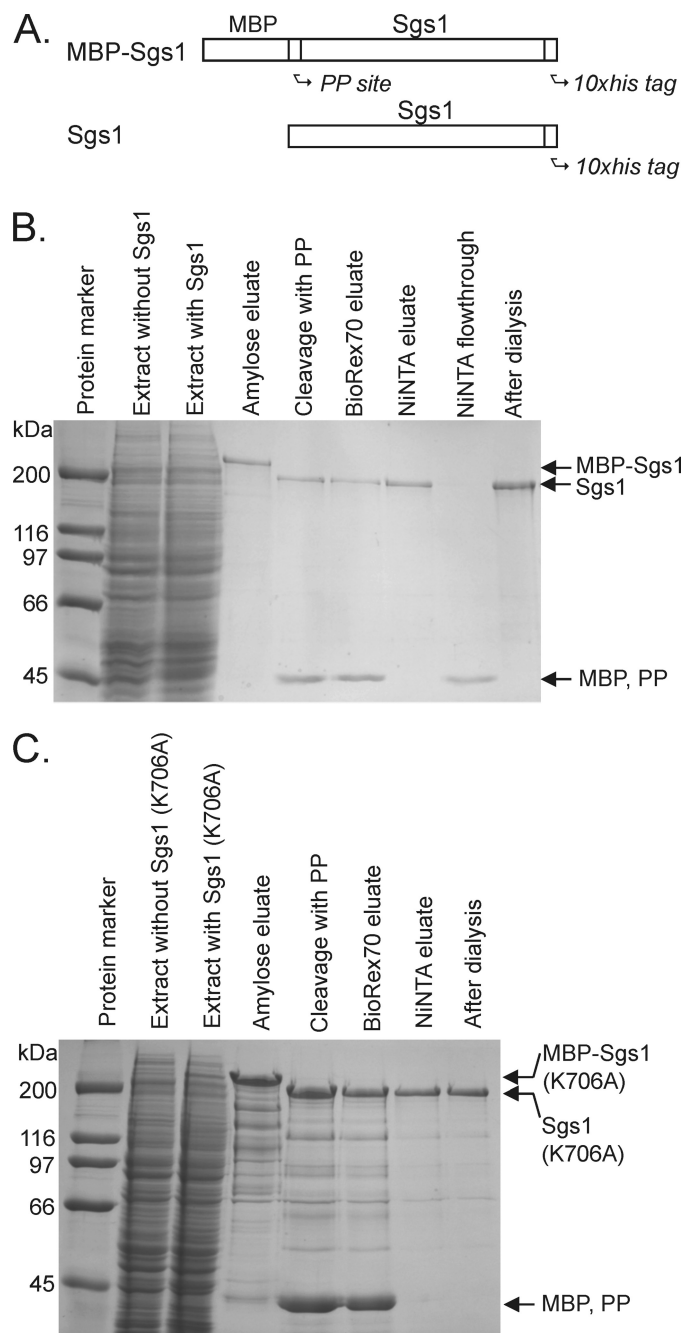
FIGURE 1. **Purification of full-length Sgs1 protein.** *A*, diagram of *SGS1* constructs. The recombinant protein was expressed in Sf9 cells with an N-terminal MBP tag and a C-terminal His$_{10}$ tag. During purification, the MBP tag was removed using PreScission protease (*PP*). Consequently, the resulting Sgs1 protein contained only the C-terminal His$_{10}$ (*10xhis*) tag. *B*, a representative Sgs1 purification showing fractions analyzed by SDS-PAGE. The positions of the recombinant constructs are indicated on the *right*, and the molecular masses of protein size markers are shown on the *left*. The gel was photographed after staining with Coomassie Brilliant Blue. *C*, fractions from the purification of the mutant, Sgs1 (K706A) protein analyzed by SDS-PAGE.

tained only the C-terminal His$_{10}$ tag and is denoted as Sgs1 (Fig. 1, *A* and *B*). The recombinant protein had a molecular mass of 166 kDa and migrated at ~200 kDa on a 6% polyacrylamide gel. The typical purification of Sgs1 (Fig. 1*B*) yielded ~100–200 μg of protein at a final concentration of ~600–900 nM. We also produced catalytically inactive Sgs1 by mutating the conserved lysine (Lys[706]) in the Walker A motif to alanine (47). The result-

ing Sgs1 (K706A) mutant was purified exactly as the wild type protein (Fig. 1*C*).

In the Absence of ATP, Sgs1 Helicase Binds to a Broad Range of DNA Substrates—We first analyzed the ability of Sgs1 to bind a diverse set of DNA substrates, using electrophoretic mobility shift assays (Fig. 2, *A* and *B*). In the absence of ATP, Sgs1 formed stable protein-DNA complexes with all of the substrates tested, although the binding to a "Y-structure" DNA substrate that contained a duplex DNA region (31 bp) and both 5'- and 3'-ssDNA tails (19 nt) showed the highest affinity (based on the midpoint, $K_d \sim 0.1$ nM), and the binding to the blunt-ended dsDNA showed the lowest affinity ($K_d \sim 3$ nM) (Fig. 2, *A* and *B*). The binding to substrates containing either a 5'- or 3'-ssDNA overhang was almost indistinguishable (Fig. 2, *A* and *B*). These results are in stark contrast to those obtained previously with the truncated Sgs1 protein, which bound exclusively to 3'-tailed DNA (36, 37). This difference suggests that the additional N- and C-terminal domains in the full-length protein potentiate DNA binding and allow the protein to bind to a wider variety of substrates. As expected, the Sgs1 (K706A) mutant possessed DNA binding activity similar to that of the wild type protein (data not shown).

Purified Full-length Sgs1 Possesses ATP Hydrolysis Activity That Is Stimulated by either ssDNA or dsDNA—The ATPase activity of the full-length Sgs1 protein was analyzed in the presence of various DNA cofactors. Sgs1 displayed a vigorous ATPase activity (Table 1) with all of the DNA substrates tested. The greatest stimulation was observed using a four-way (Holliday) junction substrate, although the longer ϕX174 ssDNA was as effective. Nearly as effective ($\sim 60-65\%$) were the Y-structure DNA, fully ssDNA, and ϕX174 dsDNA (Table 1). Both the tailed duplex DNA and the dsDNA oligonucleotide substrates stimulated Sgs1 only about one-third as well as the Holliday junction substrate.

To obtain the kinetic parameters for ATP hydrolysis, we analyzed the ATPase activity stimulated by poly(dT), which is devoid of secondary structure, as a function of increasing ATP concentration (Fig. 3*A*). The ATPase activity was hyperbolic in ATP concentration, and a fit to the data yielded $V_{max} = 1.28 \pm 0.03$ μM/s and $K_m = 43 \pm 3$ μM. Given that the Sgs1 concentration was 5 nM, the apparent k_{cat} is 256 ± 6 s^{-1}, which is an apparent ATP turnover number that is 10-fold greater than *E. coli* RecQ (48) and is comparable with that of the vigorous helicase, RecBCD (49). RPA inhibited the ATPase activity of Sgs1 by $\sim 30\%$ (Fig. 3*A*). As expected, the defective Sgs1 (K706A) mutant showed no ATPase activity (Fig. 3*A*).

Next, the DNA concentration was varied (Fig. 3*B*), resulting in the following kinetic parameters: $V_{max} = 1.31 \pm 0.10$ μM/s, $K_m = 61 \pm 11$ nM, and an apparent $k_{cat} = 263 \pm 12$ s^{-1}. Finally, when poly(dT), at a concentration (160 nM) that was greater than the K_m was used, the rate of ATP hydrolysis increased linearly with Sgs1 concentration until it saturated at an Sgs1 concentration of ~ 4.8 nM (Fig. 3*C*), corresponding to an apparent DNA-binding site size of 33 nucleotides. These parameters establish Sgs1 as a vigorous ATPase with a high apparent affinity for both ATP and ssDNA.
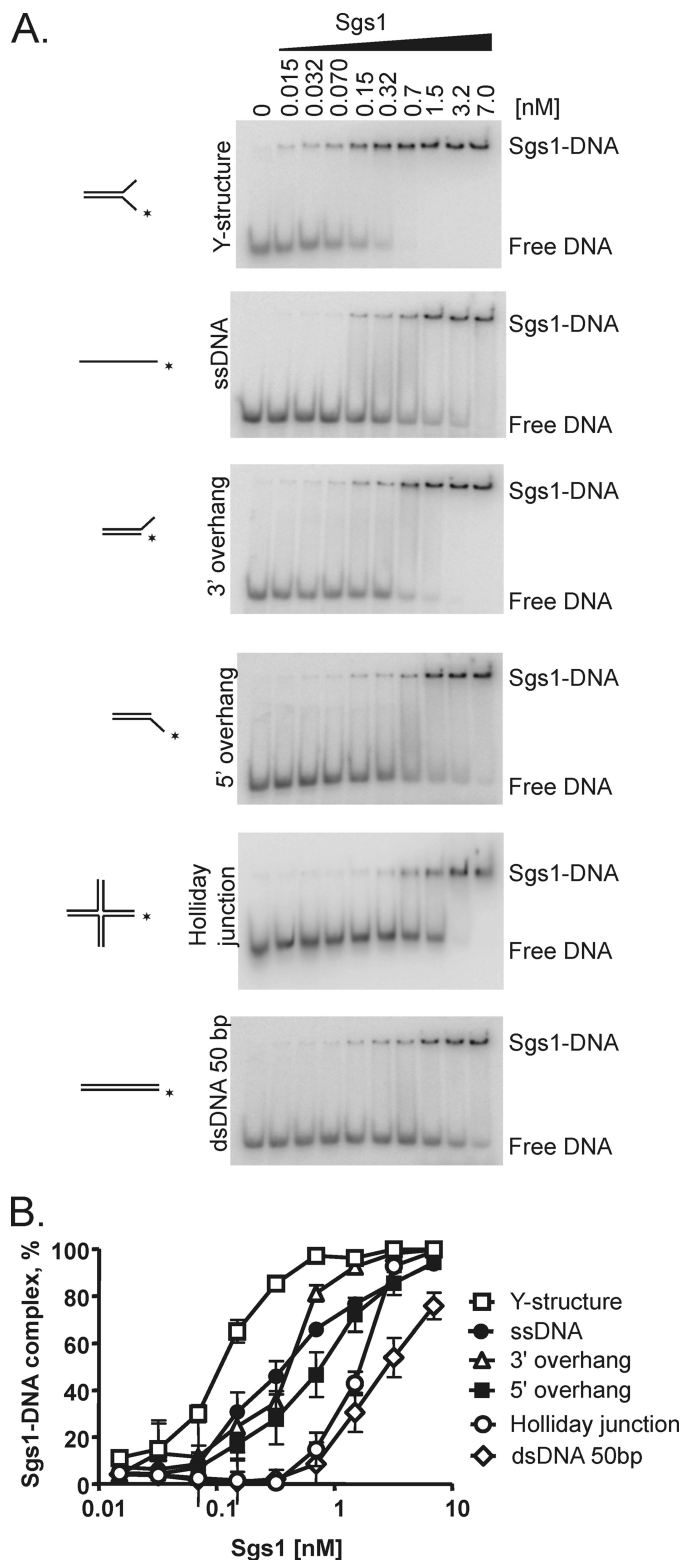
FIGURE 2. **Sgs1 binds to a broad range of DNA substrates.** *A*, electrophoretic mobility shift assays were performed as a function of Sgs1 concentrations with various DNA substrates (150 pM molecules). Shown are representative 6% polyacrylamide gels. DNA substrates are schematically depicted on the *left*. *, position of the ^{32}P label. *B*, quantification of experiments as in *A*, with the Sgs1 concentration plotted on a logarithmic scale. Data represent the average of three experiments. *Error bars*, S.E.

TABLE 1

Specificity of the ATP hydrolysis and DNA unwinding activities of full-length Sgs1 protein

ATP hydrolysis and DNA unwinding of various DNA structures are shown. DNA substrates are described under "Experimental Procedures." Values are the average of at least three experiments, and S.E. is reported. n.a., not applicable; n.d., not determined.

DNA substrate		ATP hydrolysis[a]		DNA unwinding
Description	Structure	Rate (nM·sec^{-1})[b]	apparent k_{cat} (sec^{-1})[c]	apparent K_M (pM)[d]
Holliday junction	╫	470 ± 38	235 ± 19	15 ± 1
φX174 ssDNA	◯	430 ± 45	215 ± 23	n.a.
φX174 dsDNA	◎	312 ± 27	156 ± 13	n.d.
Y-structure	⌇	304 ± 29	152 ± 15	61 ± 12
ssDNA	—	294 ± 50	147 ± 25	n.a.
dsDNA (50 bp)	═	176 ± 35	88 ± 18	122 ± 20
3'-overhang	⌐	172 ± 61	86 ± 31	146 ± 3
5'-overhang	⌐	164 ± 26	82 ± 13	135 ± 5
dsDNA (31 bp)	=	n.d.	n.d.	175 ± 3
no DNA		20 ± 6	10 ± 3	n.a.

[a] The reactions contained Sgs1 (2 nM) and the indicated DNA substrate (1 μM, nucleotides).
[b] Calculated from the linear region of the ATPase assay.
[c] Calculated by dividing the rate by the Sgs1 concentration (2 nM).
[d] Represents the Sgs1 concentration required to unwind 50% of the DNA in Fig. 5B.

Sgs1 Is a DNA Helicase That Can Be Stimulated by an ssDNA-binding Protein—The helicase activity of full-length Sgs1 was first analyzed on the Y-structure DNA substrate. Sgs1 fully unwound this substrate in a reaction that required ATP and Mg^{2+} (Fig. 4A); in contrast, the Sgs1 (K706A) mutant, which was deficient in ATP hydrolysis, showed no helicase activity (Fig. 4B). In the absence of an ssDNA-binding protein, only 24 pM Sgs1 was needed to unwind most of the substrate (150 pM molecules). However, increasing the Sgs1 concentration to 730 pM (Fig. 4A) and beyond (data not shown) actually resulted in a lower yield (~70%). A similar reduction in unwinding yield at higher protein concentrations was observed previously with several human RecQ homologues (31, 50–52) and was attributed to an apparent "DNA strand annealing" activity. Protein-mediated DNA annealing is usually the consequence of non-specific protein binding, and it occurs when DNA-binding proteins aggregate ssDNA (53). Because this apparent DNA annealing is blocked by RPA, its biological relevance remains to be determined.

Because ssDNA-binding proteins block DNA annealing, their effect on Sgs1-mediated unwinding was examined. As expected, supplementing the reaction with either *E. coli* SSB or *S. cerevisiae* RPA resulted in nearly 100% unwinding at Sgs1 concentrations at and above 240 pM (Fig. 4, *A* and *C*). Although RPA stimulated the reaction slightly better than SSB, the difference was relatively minor; in the presence of RPA, the amount
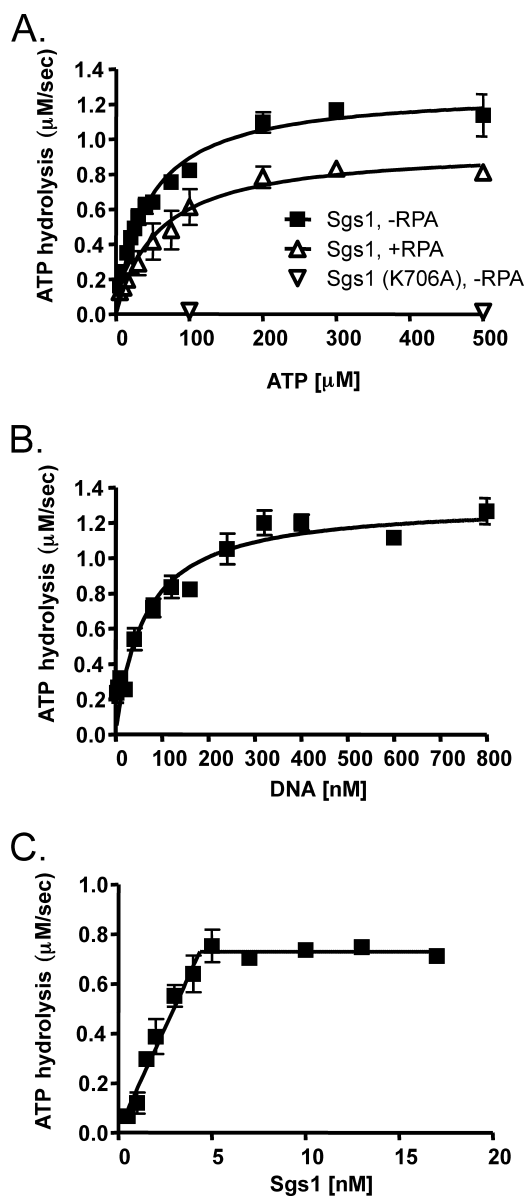

FIGURE 3. **Sgs1 shows DNA-dependent ATPase activity.** *A*, the rate of ATP hydrolysis and its dependence on ATP concentration. The reaction contained Sgs1 or Sgs1 (K706A) (5 nM), poly(dT) (1 μM nucleotides), RPA (0.15 μM; 300% of ssDNA saturation if indicated), and varying concentrations of ATP. The kinetic parameters for ATP hydrolysis (see "Results") were obtained by fitting to the Michaelis-Menten equation. *B*, the relationship between ATP hydrolysis and the concentration of DNA. The reactions contained Sgs1 (5 nM), ATP (1 mM), and the indicated concentrations of poly(dT). The kinetic parameters for ATP hydrolysis (see "Results") were obtained by fitting to the Michaelis-Menten equation. *C*, the relationship between ATP hydrolysis and Sgs1 concentration. The reactions contained poly(dT) (160 nM nucleotides), ATP (1 mM), and the concentrations of Sgs1 indicated. The data from all panels are the average of at least two independent experiments. *Error bars*, S.E.

of Sgs1 required to unwind 50% of the substrate was 50 pM, whereas in the presence of SSB, 145 pM Sgs1 was required. Therefore, we infer that both proteins are primarily acting non-specifically to bind and trap the ssDNA produced by Sgs1 helicase action and, thereby, they are preventing the reannealing of the ssDNA produced by unwinding; however, as will be seen below, the greater effectiveness of RPA may reflect a component of specific interaction between Sgs1 and RPA (54). Finally, both SSB and RPA inhibited unwinding at low Sgs1 concentra-
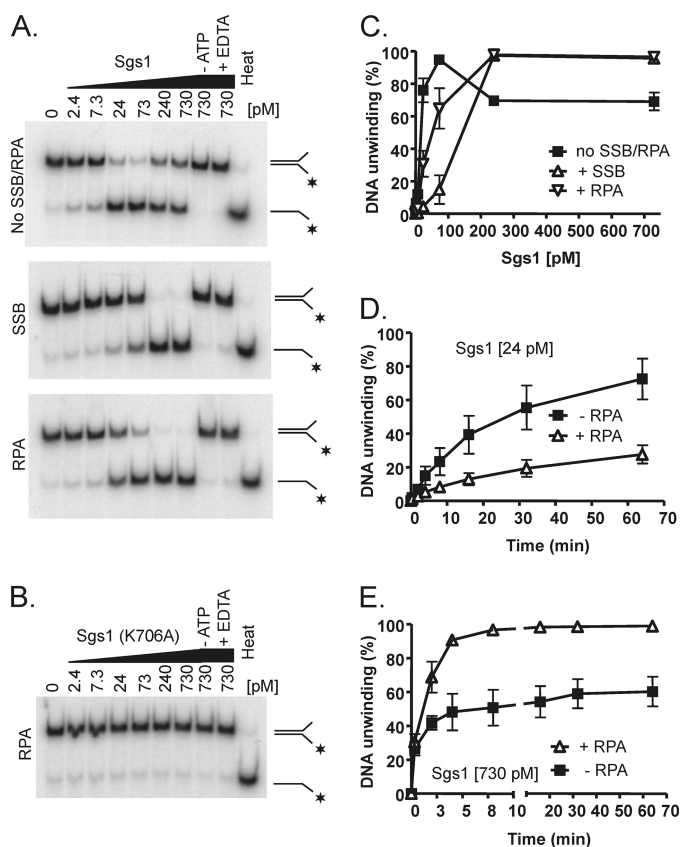
FIGURE 4. **Sgs1 is a DNA helicase.** *A,* representative polyacrylamide gels (10%) showing the DNA helicase activity of Sgs1 on a ^{32}P-labeled Y-structure DNA substrate (150 pM molecules). The substrate and reaction products are illustrated to the *right* of each gel. *, position of the ^{32}P label. Reactions were incubated for 30 min and, where indicated, supplemented with either *S. cerevisiae* RPA or *E. coli* SSB. Control reactions were as follows. *−ATP,* ATP was omitted from the reaction buffer; *+EDTA,* EDTA (33 mM) was added. The *last lane* contains heat-denatured substrate (*Heat*). *B,* analysis of the Sgs1 (K706A) mutant protein as in *A. C,* quantification of helicase assays, such as those shown in *A. D,* kinetics of unwinding of the Y-structure DNA (150 pM molecules) by 24 pM Sgs1. *E,* kinetics of unwinding of the Y-structure DNA (150 pM molecules) by 730 pM Sgs1. The results in *C–E* are the average of at least three experiments. *Error bars,* S.E.

tion (Fig. 4, *A* and *C*), suggesting competition for binding to the ssDNA tails. Similar behavior was observed for both *E. coli* RecQ (48) and human BLM (50).

We next performed a time course of the Sgs1-catalyzed DNA unwinding in the presence or absence of RPA. At a low concentration of Sgs1 (24 pM), RPA slowed the rate of unwinding ∼3-fold (Fig. 4*D*). In contrast, at high Sgs1 concentration (730 pM), RPA stimulated the reaction to result in 100% DNA unwinding within 5 min (Fig. 4*E*).

Sgs1 Helicase Unwinds a Broad Range of DNA Substrates but Prefers a Holliday Junction or Y-structure DNA—We also analyzed the ability of Sgs1 to unwind a variety of DNA substrates in the presence of RPA. We found that a four-way DNA junction, which is equivalent to a single immobile Holliday junction, was unwound most efficiently (Fig. 5, *A* and *B*), which is reminiscent of earlier observations with either BLM or WRN protein (32). To unwind 50% of the Holliday junction substrate, only about 15 pM Sgs1 was needed (Fig. 5*B*). In comparison, about 61 pM Sgs1 was required for unwinding 50% of the Y-structure DNA, the next best DNA substrate (Fig. 5*B*). Sgs1
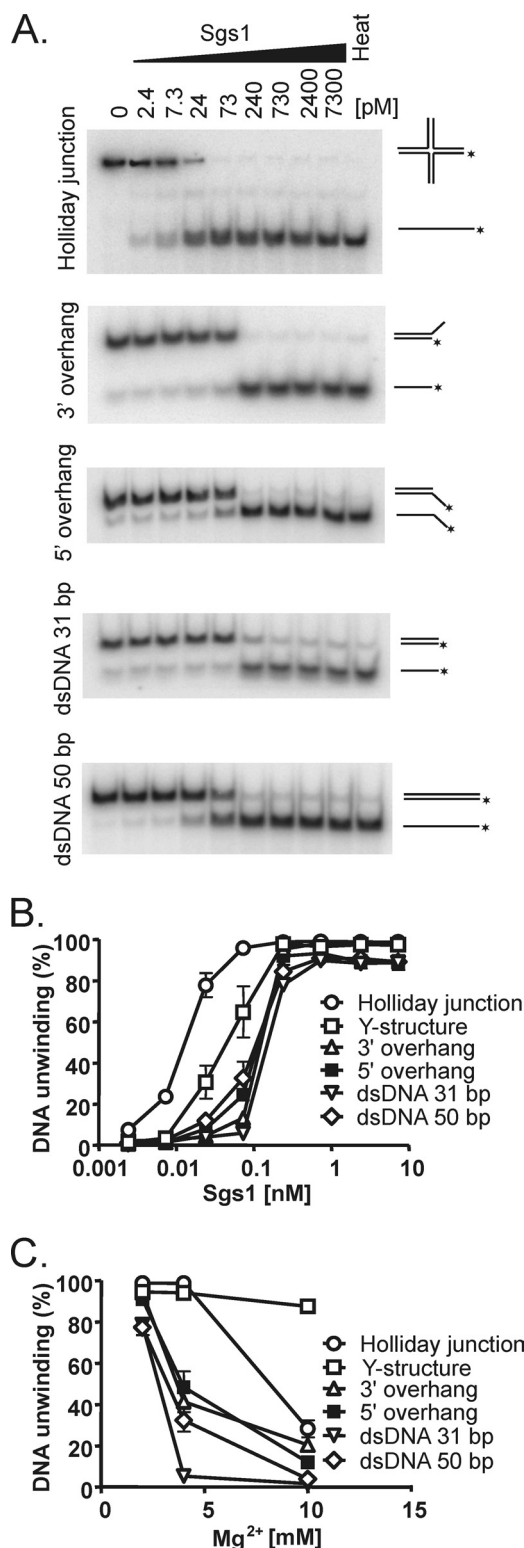

FIGURE 5. **Sgs1 can unwind a broad range of DNA substrates.** The helicase assays were carried out with the indicated ^{32}P-labeled DNA (150 pM molecules). All reactions contained RPA and were incubated for 30 min. *A,* representative polyacrylamide gels (10%) showing unwinding of four-way junction, 3′-ssDNA overhang, 5′-ssDNA overhang, 31-bp dsDNA, and 50-bp dsDNA. The substrate and product are depicted on the *right*. *, position of the ^{32}P label. The *last lane* contains heat-denatured substrate (*heat*). *B,* quantification of the helicase assays as in *A,* with the Sgs1 concentration plotted on a logarithmic scale. *C,* helicase assays at 240 pM Sgs1 carried out as in *A* as a function of magnesium acetate concentration. The results are the average of at least three experiments. *Error bars,* S.E.

could unwind all of the other substrates tested, but, compared with the Holliday junction substrate, typically 10-fold more enzyme was required to achieve the same product yield (Table 1). The unwinding of substrates containing either 5'- or 3'-ssDNA tails was almost equal over a wide range of Sgs1 concentrations (Fig. 5, *A* and *B*). Furthermore, Sgs1 did not require an ssDNA tail to initiate unwinding, because the blunt-ended duplex DNA substrate was also readily unwound (Fig. 5, *A* and *B*).

We next tested the effect of increasing Mg^{2+} concentration on the unwinding of the various substrates by Sgs1. The ability of Sgs1 to unwind blunt-ended dsDNA or substrates containing 5'- or 3'-tailed DNA dropped precipitously with increasing Mg^{2+} concentration (Fig. 5C). At 4 mM Mg^{2+}, both the Holliday junction and the Y-structure DNA were equivalent and remained at a high level. At these conditions, the selectivity for these two substrates was the highest. Interestingly, increasing the Mg^{2+} further to 10 mM revealed that the Y-structure DNA was the preferred substrate (Fig. 5C). This is probably due to a more compact structure of Holliday junction that is assumed at elevated Mg^{2+} concentrations (55). In summary, in the physiological range of Mg^{2+} concentration (1–5 mM), both Holliday junctions and Y-structure DNA are the preferred substrates for Sgs1 helicase activity, although blunt-ended dsDNA is also efficiently unwound. This behavior is reminiscent of *E. coli* RecQ (11) and is in contrast to the behavior of all of the other eukaryotic RecQ homologs (31, 32, 34, 35, 52).

The Unwinding of Substrates with Long Lengths of ssDNA Is Greatly Stimulated by RPA—We next investigated the unwinding of a ^{32}P-labeled oligonucleotide (66-mer) annealed to ϕX174 ssDNA (Fig. 6A). At concentrations greater than 7.5 nM, Sgs1 unwound 80–90% of the substrate in a reaction that required ATP and Mg^{2+} (Fig. 6B). Either SSB or RPA strongly stimulated the reactions, but, in contrast to our previous observations with the oligonucleotide-based substrates, stimulation was apparent for all Sgs1 concentrations (Fig. 6, *C–E*). As with the oligonucleotide substrates, RPA had a greater stimulatory effect than SSB, but the magnitude of the difference was larger; the concentrations of Sgs1 required for half-maximal unwinding were 16 and 50 pM with RPA and SSB, respectively, *versus* 2,500 pM in their absence, an ~150-fold and ~50-fold difference, respectively. It is also clear that in the presence of RPA, Sgs1 was acting catalytically because, for example at 24 pM Sgs1, ~75% of the substrate was unwound, indicating that one molecule of Sgs1 could unwind up to 30 substrate molecules during the 30-min reaction. The observation that RPA has a stronger stimulatory effect than SSB raises the possibility that, apart from trapping ssDNA and preventing reannealing of the ssDNA products, RPA might also stimulate Sgs1 helicase activity through specific protein-protein interaction. This is the case for human RecQ family proteins, where the helicase activity of BLM, WRN, and RecQ1 can be stimulated by a specific interaction with human RPA (56–58).

To further investigate the DNA substrate specificity of Sgs1, we prepared the substrates that had been used previously to characterize the polarity of translocation for the Sgs1 helicase domain (36). These substrates can be used to determine translocation polarity of helicases, provided that the helicase re-
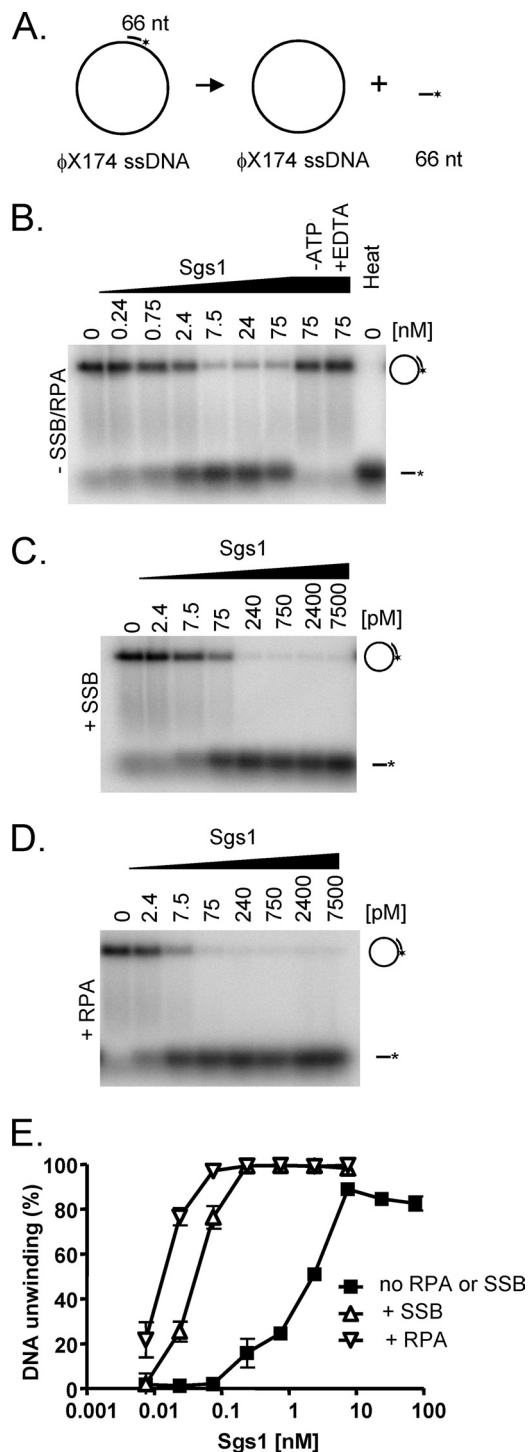
FIGURE 6. **Sgs1 can displace ssDNA annealed to ϕX174 ssDNA.** *A*, a ^{32}P-labeled oligonucleotide (66 nucleotides) was annealed to ϕX174 ssDNA (1 nM molecules) to create the substrate that was used for helicase assays; products were analyzed by electrophoresis, using agarose gels (1%). *B*, a representative gel for assays carried out without RPA or SSB for 30 min. Substrate and reaction product are depicted on the *right*. −*ATP*, control reaction where ATP was omitted; +*EDTA*, control reaction where EDTA was added at 33 mM; *heat*, heat-denatured substrate. *C*, a representative gel for the assay carried out with SSB. *D*, a representative gel for the assay carried out with RPA. *E*, quantification of at least three replicate experiments, such as those shown in *B–D*, with the Sgs1 concentration plotted on a logarithmic scale. *Error bars*, S.E.

A.

B.

C.
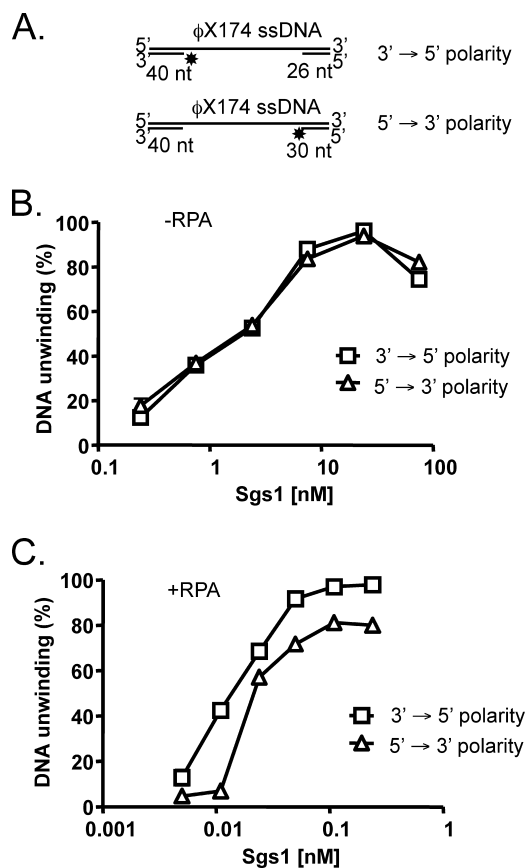
FIGURE 7. **Sgs1 displays a 3′→5′ polarity for DNA unwinding.** A helicase assay was carried out with the indicated Sgs1 concentrations and DNA substrates (1 nM molecules). *A*, a schematic representation of the DNA substrates used to define translocation polarity, 3′→5′ polarity, or 5′→3′ polarity; see "Results" for details. *B*, quantification of three replicate experiments carried out without RPA, with the Sgs1 concentration plotted on a logarithmic scale. *C*, quantification of three replicate experiments carried out with RPA, with Sgs1 concentration plotted on a logarithmic scale.

quires an ssDNA tail for unwinding. The substrates were prepared by digesting the 66-mer oligonucleotide annealed to ϕX174 ssDNA with PstI restriction endonuclease, which cuts roughly in the center of the annealed double-strand region (Fig. 7*A*). By differential labeling of the oligonucleotide at either 5′- or 3′-end, the translocation polarity of a helicase can be inferred from the displacement of one oligonucleotide fragment over the other (59), provided that the helicase cannot initiate unwinding from the blunt ends. Because full-length Sgs1 can unwind blunt-ended dsDNA (see Table 1), we examined two experimental conditions and a variety of Sgs1 concentrations. Without RPA, the unwinding of both oligonucleotide fragments by Sgs1 was identical, regardless of Sgs1 concentration (Fig. 7*B*). This is in contrast to the Sgs1 helicase domain (36), where a marked preference for unwinding of the 3′→5′-polarity substrate was observed. However, when RPA was added, differences between the two substrates were revealed. At high Sgs1 concentrations ($\geq \sim$50 pM), we could observe only a weak preference for the 3′→5′-polarity substrate (Fig. 7*C*), but, because Sgs1 displays a slight preference for a tailed substrate over the short (31-bp) blunt dsDNA substrate (Table 1), we reasoned that an unwinding bias might be revealed at lower Sgs1 concentrations. Indeed, when the concentration was re-

duced, a meaningful difference was seen at $\sim$10 pM, which, we believe, probably reveals the intrinsic preference of Sgs1 to bind the tailed ssDNA (over the alternative, the blunt dsDNA end) and to translocate in the 3′→5′ direction on ssDNA. Although these results could be interpreted to mean that Sgs1 possesses both 5′→3′ and 3′→5′ translocation directionalities, we instead conclude that these results probably reveal the intrinsic capacity of Sgs1 to translocate in the 3′→5′ direction on ssDNA, and the failure to see a large difference at the higher Sgs1 concentrations results from the ability of full-length Sgs1 to bind and unwind blunt-ended DNA duplexes. Additional translocation studies will clearly be required to determine whether this directionality is absolute, but this conclusion would also be in accord with the inferred translocation polarity of the Sgs1 helicase domain (36).

Sgs1 Can Unwind dsDNA as Long as 23 kb—The significant helicase activity of Sgs1 encouraged us to test the unwinding of longer duplex DNA molecules. To this end, we digested λ phage DNA with HindIII restriction endonuclease to generate dsDNA fragments from 0.125 to 23.1 kb in size, which were subsequently 3′-end-labeled with ^{32}P. These substrates were incubated with Sgs1 in the presence of RPA, and the reaction products were separated on a 1% agarose gel. With increasing Sgs1 concentration, the duplex DNA gradually disappeared, and novel bands appeared that correspond to the ssDNA fragments produced by heat denaturation (Fig. 8*A*). At 1.1 nM, Sgs1 unwound $\sim$80% of the longest (23.1-kb) fragment and more than 90% of the 2.3-kb fragment (Fig. 8*B*). The unwinding was dependent on ATP, Mg^{2+}, and RPA (data not shown). As expected, the Sgs1 (K706A) mutant showed no activity (data not shown). In comparison, human RECQ1 and WRN proteins are capable of unwinding only 500 and 800 bp of duplex DNA, respectively (57, 58), and BLM could partially unwind a 259-bp duplex but not an 851-bp duplex (56). These results show that Sgs1 is a far more capable helicase than any of other eukaryotic RecQ homologues.

DISCUSSION

The wild type full-length Sgs1 protein from *S. cerevisiae* contains 1447 amino acids, making it one of the largest members of the RecQ family of helicases. Previous attempts to produce full-length Sgs1 failed, mainly due to insolubility of the overexpressed protein. Instead, the central domain containing amino acids 400–1268 of Sgs1 was characterized (36, 37). Although this protein fragment possesses helicase and ATPase activities, it lacks the considerable N- and C-terminal domains that might influence the specificity and activity of the helicase. We overcame the solubility problems by fusing Sgs1 with MBP and by expressing the construct in insect cells using a baculovirus expression system. Consequently, we could provide the first biochemical characterization of full-length Sgs1 protein.

Our experiments revealed that, as expected for an RecQ homolog, Sgs1 is a DNA-dependent ATPase as well as a DNA helicase. However, unlike the other eukaryotic RecQ homologues, Sgs1 shows a broad substrate specificity and is remarkably active. The apparent k_{cat} for ATP hydrolysis in the presence of ssDNA is $\sim$260 s^{-1}, which is about 26-fold higher than that of the helicase domain (36). For comparison, the k_{cat} values

A.

B.
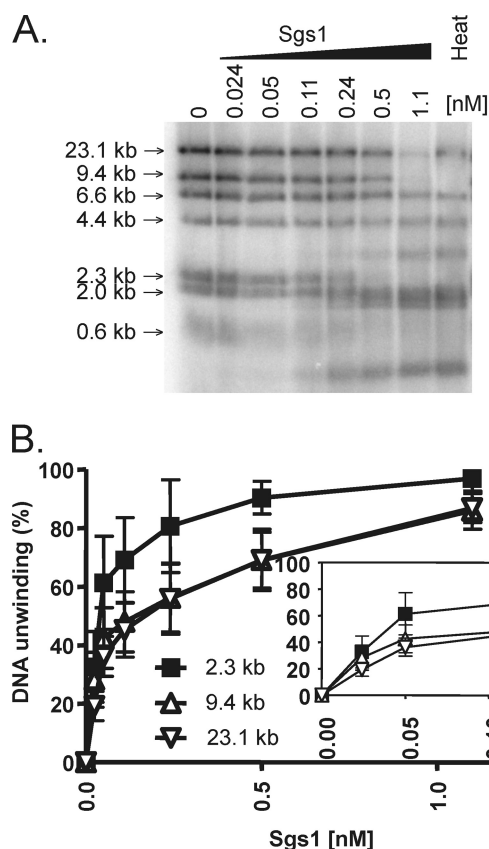
FIGURE 8. **Sgs1 can unwind long lengths of dsDNA.** *A*, λ phage DNA was digested with HindIII and ^{32}P-labeled with Klenow fragment of DNA polymerase I at the 3′-ends. This substrate (each fragment at 50 pM molecules) was used for helicase assays at the indicated Sgs1 concentrations. The reactions were carried out in the presence of RPA. Sizes of the dsDNA substrates are indicated on the *left*. *Heat*, heat-denatured substrate. The *panel* shows a representative agarose gel (1%). *B*, quantification of unwinding of the 23.1-, 9.4-, and 2.3-kb DNA fragments. The quantification was based on the disappearance of the bands corresponding to the respective dsDNA fragment. The results are the average of three experiments. *Error bars*, S.E.

for ssDNA-dependent ATP hydrolysis for *E. coli* RecQ, human BLM, human WRN, and human RECQ1 are 24, 2.4–19, 1.0–2.5, and 2.1 s^{-1}, respectively (48, 56–58), making Sgs1 10–100-fold more active than other members of the RecQ helicase family.

Sgs1 exhibits a strong DNA binding and DNA unwinding activity. In the absence of ATP, the full-length Sgs1 binds a variety of oligonucleotide-based substrates; it shows a preference for the Y-structure DNA, binds DNA with 5′- or 3′-ssDNA overhangs indiscriminately, and binds blunt-ended duplex DNA with the lowest affinity (Fig. 2). As a result, full-length Sgs1 can unwind all of the substrates tested. However, perhaps because the helicase assays contain ATP, the full-length Sgs1 shows a distinct preference for the single Holliday junction and the Y-structure DNA (Figs. 4 and 5), and it unwinds these substrates with K_m values that are 15 and 61 pM, respectively (Table 1).

Somewhat unexpectedly, Sgs1 resembles the *E. coli* RecQ helicase more than any of the human RecQ family members. RecQ was shown to bind a wide variety of substrates with relatively low differences in affinity (11) (*e.g.* Y-structure DNA is bound 8-fold better than duplex DNA, which is com-

parable with what we observe with Sgs1) (Fig. 2). The differences in unwinding rates for various DNA substrates were typically smaller than for DNA binding affinities (11), again similar to the behavior of Sgs1 (Fig. 5). Furthermore, Sgs1 can unwind all of the oligonucleotide-based substrates with K_m values that range from 15 to 180 pM. In contrast, BLM, the closest human homologue, can unwind only a Holliday junction, Y-structure DNA, and, to a limited level, dsDNA with a 3′-ssDNA overhang; this unwinding requires at least 20 nM BLM (32). We estimate the rate of DNA unwinding by Sgs1 to range from 6 to 30 bp/s, based on results from Fig. 8 and further unpublished observations.[3] Due to the complex DNA binding properties of Sgs1 and the competition with RPA for ssDNA binding, properties that are shared by the *E. coli* RecQ (48), a more detailed analysis of unwinding rates is beyond the scope of this paper.

There are notable differences between the Sgs1 helicase domain fragment and the full-length protein. With regard to DNA binding specificity, the helicase domain of Sgs1 binds ssDNA, DNA containing branched structures, and DNA with a 3′-ssDNA overhang. It was concluded that this binding specificity determines the 3′→5′ polarity of DNA unwinding (37). In contrast to the full-length Sgs1, the helicase domain can unwind dsDNA oligonucleotide substrates with either Y-structure or 3′-ssDNA tails but not dsDNA with blunt ends or a 5′-ssDNA tail (36, 37). Importantly, we observed dramatic differences between full-length Sgs1 and Sgs1 helicase domain with regard to quantitative aspects of DNA binding and unwinding. To bind ~50% of dsDNA with a 3′-ssDNA tail, the best substrate for the Sgs1 helicase domain, 30 nM protein is needed (37). In contrast, only 0.46 nM full-length Sgs1 was required to achieve comparable binding (Fig. 2). Similar differences were observed for the helicase activity as well.

The marked differences between the two proteins suggest that the N- and C-terminal regions contain auxiliary DNA binding domains that enable Sgs1 to bind and unwind a wider spectrum of DNA substrates. It is likely that, due to the relatively low affinity of the Sgs1 helicase domain for DNA, the concentration of protein required for binding and unwinding of duplex DNA could not be reached. One of the domains that is likely to potentiate Sgs1 function is the HRDC domain. The HRDC domain is present in a number of eukaryotic RecQ homologues, although it is not essential for helicase activity. Structural studies showed that the HRDC domain resembles the auxiliary helicase domains of bacterial DNA helicases and suggested that it might interact with DNA (39, 40). The HRDC domain in BLM is required for the dissolution of Holliday junctions, and it was proposed to confer DNA structure specificity (24).

In addition, the C terminus of Sgs1 probably contains an ssDNA binding capacity. Human BLM, RECQ4, RECQ5β, and WRN proteins (31, 50–52) can anneal complementary ssDNA when RPA is absent. It seems likely that the annealing activity is a result of nonspecific ssDNA binding, because the C-terminal domain of BLM binds and anneals ssDNA, but this annealing

---

[3] P. Cejka and S. C. Kowalczykowski, unpublished observations.

activity is blocked by an ssDNA-binding protein (50). Although here we did not seek to characterize the DNA annealing capability of Sgs1, we observed that high concentrations of Sgs1 partially reduce the extent of DNA unwinding (Fig. 4*A*). In the case of the human RecQ homologues, this behavior is indicative of DNA annealing activity but is not a characteristic of the Sgs1 helicase domain. Collectively, these data suggest that the full-length protein contains additional domains that facilitate DNA binding. The N- and C-terminal regions promote the binding to and unwinding of DNA and thus explain the differences in substrate specificity between the helicase domain and the full-length proteins.

Previous genetic and biochemical studies established that a subset of the functions of certain RecQ family helicases is mediated by the species-specific interaction with topoisomerase III homologs (2, 18, 23, 60). These interactions are conserved from bacteria to humans. The Rmi1 protein was discovered later as an additional component of the heterotrimeric functional complex (61, 62). The major role of this concerted helicase-topoisomerase complex is to catenate or decatenate dsDNA, resulting in the resolution or "dissolution" of double Holliday junctions at the final steps of homologous recombination. Human and *Drosophila* BLM proteins were shown to function with topoisomerase IIIα to convergently migrate two Holliday junctions, ultimately leading to the separation of the two joined molecules (22, 23). Based on genetic evidence (9, 21), Sgs1 is expected to participate in similar reactions. Our observation, showing that a single Holliday junction was the preferred substrate for Sgs1 helicase and ATPase activities, further supports this hypothesis.

More recent genetic data defined an additional important role for Sgs1 early in recombination. Following the formation of a double-stranded DNA break, Sgs1 is involved in the resection of dsDNA (27–29) to produce an extended 3′-ssDNA tail that serves as the substrate for recombination. The helicase activity of Sgs1 is required for end resection, as are the nucleases Dna2 and exonuclease 1 (28). Biochemical studies established that the BLM helicase stimulated resection of dsDNA by exonuclease 1 to create a substrate for homologous pairing by the DNA strand exchange protein, RAD51 (30). Related biochemical analyses with a reconstituted reaction of *E. coli* proteins revealed the RecQ-stimulated resection of dsDNA by the RecJ exonuclease (12). *In vivo*, resection tracks as long as 20 kb were observed (28). Our data, showing that Sgs1 can unwind similarly large DNA duplexes (Fig. 8), suggest that such a function of Sgs1 is conceivable.

In summary, we show that Sgs1 is a remarkably active helicase that acts on a broad range of DNA molecules, making it an appropriate helicase in the resection stage of recombination. Furthermore, consistent with its additional role in the resolution stage of recombination, Sgs1 shows a preference for unwinding Holliday junctions. We are further investigating the mechanistic aspects of Holliday junction unwinding, and because this analysis is very complex, it is beyond the scope of this report and will be reported elsewhere. The full-length Sgs1 protein will be indispensable in the biochemical characterization of Sgs1 in other aspects of DNA metabolism.

REFERENCES

1. Nakayama, H., Nakayama, K., Nakayama, R., Irino, N., Nakayama, Y., and Hanawalt, P. C. (1984) *Mol. Gen. Genet.* **195,** 474–480
2. Gangloff, S., McDonald, J. P., Bendixen, C., Arthur, L., and Rothstein, R. (1994) *Mol. Cell. Biol.* **14,** 8391–8398
3. Watt, P. M., Louis, E. J., Borts, R. H., and Hickson, I. D. (1995) *Cell* **81,** 253–260
4. Wu, L., and Hickson, I. D. (2006) *Annu. Rev. Genet.* **40,** 279–306
5. Ellis, N. A., Groden, J., Ye, T. Z., Straughen, J., Lennon, D. J., Ciocci, S., Proytcheva, M., and German, J. (1995) *Cell* **83,** 655–666
6. Yu, C. E., Oshima, J., Fu, Y. H., Wijsman, E. M., Hisama, F., Alisch, R., Matthews, S., Nakura, J., Miki, T., Ouais, S., Martin, G. M., Mulligan, J., and Schellenberg, G. D. (1996) *Science* **272,** 258–262
7. Kitao, S., Shimamoto, A., Goto, M., Miller, R. W., Smithson, W. A., Lindor, N. M., and Furuichi, Y. (1999) *Nat. Genet.* **22,** 82–84
8. Ouyang, K. J., Woo, L. L., and Ellis, N. A. (2008) *Mech. Ageing Dev.* **129,** 425–440
9. Mankouri, H. W., and Hickson, I. D. (2007) *Trends Biochem. Sci.* **32,** 538–546
10. Umezu, K., Nakayama, K., and Nakayama, H. (1990) *Proc. Natl. Acad. Sci. U.S.A.* **87,** 5363–5367
11. Harmon, F. G., and Kowalczykowski, S. C. (1998) *Genes Dev.* **12,** 1134–1144
12. Handa, N., Morimatsu, K., Lovett, S. T., and Kowalczykowski, S. C. (2009) *Genes Dev.* **23,** 1234–1245
13. Kowalczykowski, S. C. (2000) *Trends Biochem. Sci.* **25,** 156–165
14. Spies, M., and Kowalczykowski, S. C. (2005) in *The Bacterial Chromosome* (Higgins, N. P., ed) pp. 389–403, American Society for Microbiology Press, Washington, D. C.
15. Kuzminov, A. (1999) *Microbiol. Mol. Biol. Rev.* **63,** 751–813
16. Ryder, L., Whitby, M. C., and Lloyd, R. G. (1994) *J. Bacteriol.* **176,** 1570–1577
17. Hanada, K., Ukita, T., Kohno, Y., Saito, K., Kato, J., and Ikeda, H. (1997) *Proc. Natl. Acad. Sci. U.S.A.* **94,** 3860–3865
18. Harmon, F. G., DiGate, R. J., and Kowalczykowski, S. C. (1999) *Mol. Cell* **3,** 611–620
19. Harmon, F. G., Brockman, J. P., and Kowalczykowski, S. C. (2003) *J. Biol. Chem.* **278,** 42668–42678
20. Suski, C., and Marians, K. J. (2008) *Mol. Cell* **30,** 779–789
21. Liberi, G., Maffioletti, G., Lucca, C., Chiolo, I., Baryshnikova, A., Cotta-Ramusino, C., Lopes, M., Pellicioli, A., Haber, J. E., and Foiani, M. (2005) *Genes Dev.* **19,** 339–350
22. Plank, J. L., Wu, J., and Hsieh, T. S. (2006) *Proc. Natl. Acad. Sci. U.S.A.* **103,** 11118–11123
23. Wu, L., and Hickson, I. D. (2003) *Nature* **426,** 870–874
24. Wu, L., Chan, K. L., Ralf, C., Bernstein, D. A., Garcia, P. L., Bohr, V. A., Vindigni, A., Janscak, P., Keck, J. L., and Hickson, I. D. (2005) *EMBO J.* **24,** 2679–2687
25. Adams, M. D., McVey, M., and Sekelsky, J. J. (2003) *Science* **299,** 265–267
26. Myung, K., Datta, A., Chen, C., and Kolodner, R. D. (2001) *Nat. Genet.* **27,** 113–116
27. Gravel, S., Chapman, J. R., Magill, C., and Jackson, S. P. (2008) *Genes Dev.* **22,** 2767–2772
28. Zhu, Z., Chung, W. H., Shim, E. Y., Lee, S. E., and Ira, G. (2008) *Cell* **134,** 981–994
29. Mimitou, E. P., and Symington, L. S. (2008) *Nature* **455,** 770–774
30. Nimonkar, A. V., Ozsoy, A. Z., Genschel, J., Modrich, P., and Kowalczykowski, S. C. (2008) *Proc. Natl. Acad. Sci. U.S.A.* **105,** 16906–16911
31. Garcia, P. L., Liu, Y., Jiricny, J., West, S. C., and Janscak, P. (2004) *EMBO J.*

23, 2882–2891

32. Mohaghegh, P., Karow, J. K., Brosh Jr., R. M., Jr., Bohr, V. A., and Hickson, I. D. (2001) *Nucleic Acids Res.* **29,** 2843–2849
33. Huber, M. D., Lee, D. C., and Maizels, N. (2002) *Nucleic Acids Res.* **30,** 3954–3961
34. Orren, D. K., Brosh, R. M., Jr., Nehlin, J. O., Machwe, A., Gray, M. D., and Bohr, V. A. (1999) *Nucleic Acids Res.* **27,** 3557–3566
35. Popuri, V., Bachrati, C. Z., Muzzolini, L., Mosedale, G., Costantini, S., Giacomini, E., Hickson, I. D., and Vindigni, A. (2008) *J. Biol. Chem.* **283,** 17766–17776
36. Bennett, R. J., Sharp, J. A., and Wang, J. C. (1998) *J. Biol. Chem.* **273,** 9644–9650
37. Bennett, R. J., Keck, J. L., and Wang, J. C. (1999) *J. Mol. Biol.* **289,** 235–248
38. Wu, L., Davies, S. L., Levitt, N. C., and Hickson, I. D. (2001) *J. Biol. Chem.* **276,** 19375–19381
39. Liu, Z., Macias, M. J., Bottomley, M. J., Stier, G., Linge, J. P., Nilges, M., Bork, P., and Sattler, M. (1999) *Structure Fold Des* **7,** 1557–1566
40. Bernstein, D. A., Zittel, M. C., and Keck, J. L. (2003) *EMBO J.* **22,** 4910–4921
41. Kantake, N., Sugiyama, T., Kolodner, R. D., and Kowalczykowski, S. C. (2003) *J. Biol. Chem.* **278,** 23410–23417
42. Whitby, M. C., and Lloyd, R. G. (1998) *J. Biol. Chem.* **273,** 19729–19739
43. Kumaran, S., Kozlov, A. G., and Lohman, T. M. (2006) *Biochemistry* **45,** 11958–11973
44. Lohman, T. M., and Ferrari, M. E. (1994) *Annu. Rev. Biochem.* **63,** 527–570
45. Kreuzer, K. N., and Jongeneel, C. V. (1983) *Methods Enzymol.* **100,** 144–160
46. Kowalczykowski, S. C., and Krupp, R. A. (1987) *J. Mol. Biol.* **193,** 97–113
47. Lo, Y. C., Paffett, K. S., Amit, O., Clikeman, J. A., Sterk, R., Brenneman, M. A., and Nickoloff, J. A. (2006) *Mol. Cell. Biol.* **26,** 4086–4094
48. Harmon, F. G., and Kowalczykowski, S. C. (2001) *J. Biol. Chem.* **276,** 232–243
49. Roman, L. J., and Kowalczykowski, S. C. (1989) *Biochemistry* **28,** 2873–2881
50. Cheok, C. F., Wu, L., Garcia, P. L., Janscak, P., and Hickson, I. D. (2005) *Nucleic Acids Res.* **33,** 3932–3941
51. Machwe, A., Xiao, L., Groden, J., Matson, S. W., and Orren, D. K. (2005) *J. Biol. Chem.* **280,** 23397–23407
52. Macris, M. A., Krejci, L., Bussen, W., Shimamoto, A., and Sung, P. (2006) *DNA Repair* **5,** 172–180
53. Kowalczykowski, S. C., and Eggleston, A. K. (1994) *Annu. Rev. Biochem.* **63,** 991–1043
54. Cobb, J. A., Bjergbaek, L., Shimada, K., Frei, C., and Gasser, S. M. (2003) *EMBO J.* **22,** 4325–4336
55. McKinney, S. A., Déclais, A. C., Lilley, D. M., and Ha, T. (2003) *Nat. Struct. Biol.* **10,** 93–97
56. Brosh, R. M., Jr., Li, J. L., Kenny, M. K., Karow, J. K., Cooper, M. P., Kureekattil, R. P., Hickson, I. D., and Bohr, V. A. (2000) *J. Biol. Chem.* **275,** 23500–23508
57. Brosh, R. M., Jr., Orren, D. K., Nehlin, J. O., Ravn, P. H., Kenny, M. K., Machwe, A., and Bohr, V. A. (1999) *J. Biol. Chem.* **274,** 18341–18350
58. Cui, S., Arosio, D., Doherty, K. M., Brosh, R. M., Jr., Falaschi, A., and Vindigni, A. (2004) *Nucleic Acids Res.* **32,** 2158–2170
59. Matson, S. W. (1986) *J. Biol. Chem.* **261,** 10169–10175
60. Bennett, R. J., Noirot-Gros, M. F., and Wang, J. C. (2000) *J. Biol. Chem.* **275,** 26898–26905
61. Mullen, J. R., Nallaseth, F. S., Lan, Y. Q., Slagle, C. E., and Brill, S. J. (2005) *Mol. Cell. Biol.* **25,** 4476–4487
62. Chang, M., Bellaoui, M., Zhang, C., Desai, R., Morozov, P., Delgado-Cruzata, L., Rothstein, R., Freyer, G. A., Boone, C., and Brown, G. W. (2005) *EMBO J.* **24,** 2024–2033